JCI insight

RESEARCH ARTICLE

Cigarette smoke–induced reduction of C1q promotes emphysema

Xiaoyi Yuan,[1] Cheng-Yen Chang,[1] Ran You,[1] Ming Shan,[1] Bon Hee Gu,[1] Matthew C. Madison,[1] Gretchen Diehl,[2] Sarah Perusich,[1] Li-Zhen Song,[1] Lorraine Cornwell,[3] Roger D. Rossen,[4] Rick Wetsel,[5] Rajapakshe Kimal,[6] Cristian Coarfa,[6] Holger K. Eltzschig,[7] David B. Corry,[1,4,8,9] and Farrah Kheradmand[1,4,6,8,9]

[1]Department of Medicine, Pulmonary and Critical Care, Baylor College of Medicine, Houston, Texas, USA. [2]Department of Molecular Virology and Microbiology Baylor College of Medicine, Houston, Texas, USA. [3]Department of Surgery, Baylor College of Medicine, Houston, Texas, USA. [4]Center for Translational Research in Inflammatory Diseases, Michael E. DeBakey VA, Houston, Texas, USA. [5]Institute of Molecular Medicine, UT Health Science Center of Houston, Houston, Texas, USA. [6]Department of Molecular and Cell Biology, Baylor College of Medicine, Houston, Texas, USA. [7]Department of Anesthesiology, UT Health Science Center at Houston, Houston, Texas, USA. [8]Departments of Pathology and Immunology, Baylor College of Medicine, Houston, Texas, USA. [9]Biology of Inflammation Center, Baylor College of Medicine, Houston, Texas, USA.

Alteration of innate immune cells in the lungs can promote loss of peripheral tolerance that leads to autoimmune responses in cigarette smokers. Development of autoimmunity in smokers with emphysema is also strongly linked to the expansion of autoreactive T helper (Th) cells expressing interferon γ (Th1), and interleukin 17A (Th17). However, the mechanisms responsible for enhanced self-recognition and reduced immune tolerance in smokers with emphysema remain less clear. Here we show that C1q, a component of the complement protein 1 complex (C1), is downregulated in lung CD1a$^+$ antigen-presenting cells (APCs) isolated from emphysematous human and mouse lung APCs after chronic cigarette smoke exposure. C1q potentiated the function of APCs to differentiate CD4$^+$ T cells to regulatory T cells (Tregs), while it inhibited Th17 cell induction and proliferation. Mice deficient in C1q that were exposed to chronic smoke exhibited exaggerated lung inflammation marked by increased Th17 cells, whereas reconstitution of C1q in the lungs enhanced Treg abundance, dampened smoke-induced lung inflammation, and prevented the development of emphysema. Our findings demonstrate that cigarette smoke–mediated loss of C1q could play a key role in reduced peripheral tolerance, which could be explored to treat emphysema.

Introduction

Exposure to chronic cigarette smoke and the particulate matter derived from the incomplete combustion of tobacco (e.g., nano-sized carbon black) can cause irreversible destruction of the lung parenchyma, termed emphysema, a form of chronic obstructive pulmonary disease (COPD; refs. 1–4). The pathogenesis of pulmonary emphysema, an endotype of smoke-induced inflammatory lung diseases that is associated with high morbidity and affects a subset of smokers, remains incompletely understood. COPD and lung destruction can manifest heterogeneously among subjects with similar smoking histories, indicating that several predisposing factors may play pathogenic roles in disease initiation and/or progression (5, 6). In addition to chronic lung diseases and cancer, smokers are at increased risk for the development of systemic autoinflammation affecting different organs that can progress despite smoking cessation, suggesting that cigarette smoke could also mediate loss of peripheral tolerance in susceptible individuals (7–11).

Antigen-presenting cells (APCs), macrophages, and CD1a$^+$ conventional dendritic cells (cDCs), isolated from emphysematous lungs, can promote differentiation of autoreactive T helper 1 (Th1) and Th17 cells that express interferon γ (IFN-γ) and interleukin 17A (IL-17A), respectively (12, 13). We have shown that in response to chronic smoke exposure, mouse lung CD11b$^+$/CD11c$^+$ APCs upregulate costimulatory molecules (e.g., MHC-II, CD86) that can induce differentiation of Th1 and Th17 cells in vitro (13). Smoke exposure elicits activated APCs in the lungs, and adoptive transfer of CD11b$^+$/CD11c$^+$ cells (cDCs) from the lungs of smoke-exposed mice induces intense lung inflammation and emphysema in naive mice (4, 13).

Conflict of interest: Conflict of interest:

Submitted: August 17, 2018
Accepted: May 16, 2019
Published: July 11, 2019.

Reference information: *JCI Insight*. 2019;4(13):e124317. https://doi.org/10.1172/jci.insight.124317.

In addition, adoptive transfer of T cells derived from mice exposed chronically to smoke also induces emphysema in non-exposed mice (14). These findings highlight the critical role of innate and adaptive immunity in the pathophysiology of cigarette smoke–induced emphysema.

Epidemiological studies have also shown a strong risk factor between the induction of several classic autoimmune and autoinflammatory diseases including rheumatoid arthritis (15), systemic lupus erythematosus (SLE; ref. 16), and vasculitis (17) in human smokers. Smokers with emphysema also manifest increased circulating anti-nuclear and other self-reactive antibodies in addition to autoreactive T cells reacting especially to elastin, a major matrix protein of the lung (18–20). Although these studies strongly implicate cigarette smoke in the loss of self-tolerance that predisposes to the development of such autoimmune inflammation, the essential underlying mechanism(s) in susceptible smokers by which this occurs remain poorly understood.

Complement proteins are critical modifiers of innate and acquired immunity (21, 22). We have shown that in response to cigarette smoke, mice deficient in C3 ($C3^{-/-}$) or the receptor for the active C3a fragment ($C3ar^{-/-}$) recruit fewer cDCs to the lungs, show attenuated Th17 cell inflammation, and are protected against emphysema development (23). In addition, cigarette smoke–induced induction of endogenous serine and matrix metalloproteinases (e.g., cathepsins, MMP9, MMP12) in innate immune cells can result in the cleavage and activation of C3 to yield C3a to further amplify proinflammatory functions of cDCs in vivo (23).

In addition to these endogenous proteinases, C1q, as a component of the C1 complex that consists of C1q, C1r, and C1s, also activates C3 via the classic, antibody-dependent complement activation pathway (24–26). Paradoxically, primary or secondary loss of C1q and/or its reduced bioavailability of heterologous domains (e.g., C1qa, C1qb, or C1qc) which is highly conserved between species, are linked to several autoinflammatory diseases (27–29). These findings indicate that C1q proteins could play complex roles in the activation of innate and adaptive immunity that is linked to autoinflammation, but its precise role in cigarette smoke–induced emphysema remains unknown.

C1q is predominantly secreted by APCs (cDCs and macrophages; refs. 30, 31) and microglia (32). At age 6 to 8 months, mice with global deficiency of C1q ($C1qa^{-/-}$) develop anti-nuclear antibodies that result in severe autoinflammation-mediated nephritis, reminiscent of genetic or acquired loss of C1q in SLE patients (33). Anti-C1q antibody titers and Treg numbers negatively correlate in SLE patients (34), suggesting that C1q is protective in autoinflammation. In addition, bone marrow–derived APCs isolated from $C1qa^{-/-}$ mice express more IL12p40 in response to lipopolysaccharide compared with wild-type (WT) cells (35), indicating that immune responses to bacterial pathogens are dysregulated in the absence of C1q. Although these findings strongly support an association between C1q expression and induction of autoimmune responses, a link between dysregulation of C1q and reduced immune tolerance in response to cigarette smoke remains unclear.

In this study, we examined the significance of C1q in the loss of immune tolerance in response to cigarette smoke. Lung APCs from smokers and mice exposed to chronic cigarette smoke showed reduced C1q expression. We explored the function of C1q using an in vivo model of smoke-exposed emphysema and in vitro T cell differentiation studies. Mechanistically we show how C1q induces Treg differentiation, a pathway that could be used as a therapeutic target in smoke-induced autoimmune inflammation.

Results

Emphysema APCs show reduced C1q expression. To understand how C1q potentially contributes to the pathogenesis of emphysema, we initially performed whole transcriptome analyses of $CD1a^+$ APCs isolated from the lungs of human smokers with and without emphysema as previously published (ref. 36; GSE26296). This analysis revealed an approximately 50% reduction in *C1Q* mRNA in smokers with emphysema compared with emphysema-free control smokers (Figure 1A and Supplemental Figure 1; supplemental material available online with this article; https://doi.org/10.1172/jci.insight.124317DS1). Lung $CD1a^+$ APCs, isolated from a different group, confirmed reduced expression of *C1QA* in smokers with emphysema; current smokers also showed a significantly reduced *C1QA* expression compared with former smokers (Figure 1, B and C). In addition, linear regression analysis showed that *C1QA* gene expression and plasma C1q concentration negatively correlated with the severity of lung obstruction as measured by forced expiratory volume in 1 second (FEV_1) and airflow obstruction (Figure 1D and Supplemental Figure 2, A and B). The correlation between plasma C1q concentration and emphysema severity also showed a significant linear regression (Supplemental Figure 2C). Similarly, smokers with emphysema showed significantly reduced

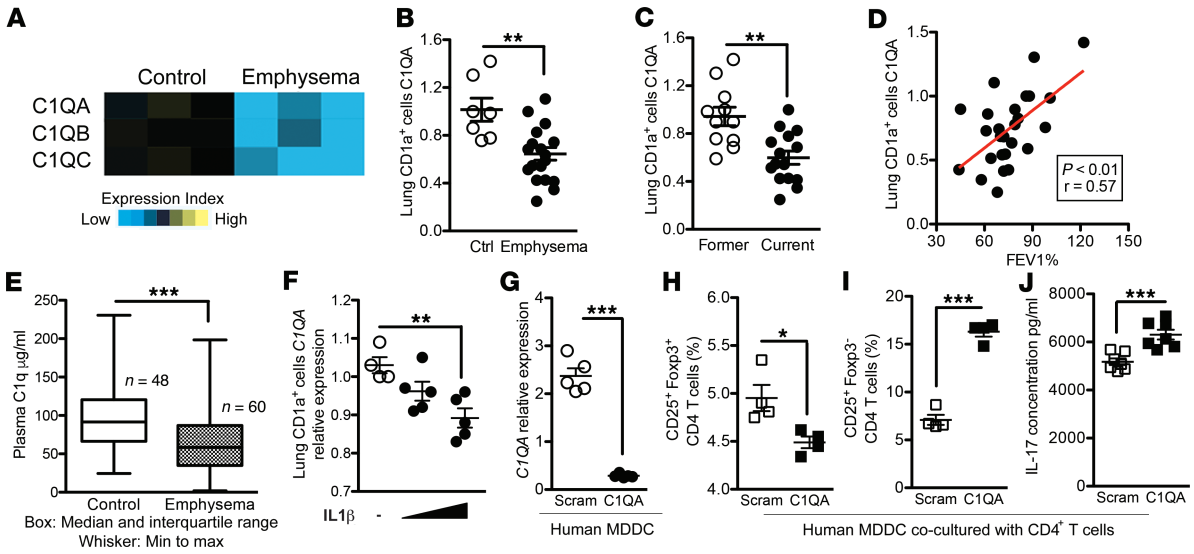

Figure 1. mRNA expression and protein concentration of C1q are reduced in human emphysema. (**A**) Heatmap using microarray of C1q expression in lung CD1a⁺ cells isolated from control and emphysema patients (GSE26296). (**B**) Expression of *C1QA* mRNA in CD1a⁺ APCs isolated from total lung cells was measured by qPCR (normalized to *18S* expression). Ctrl, control (smokers without emphysema); $N = 26$. (**C**) The same data were used to separate subjects based on current (active) vs. former (>1 year inactive) smoking history. $^{**}P < 0.01$. (**D**) Linear regression was used to find the correlation between *C1QA* mRNA in CD1a⁺ APCs and airway obstruction as measured by lung function (% forced expiratory volume in 1 second; FEV_1). (**E**) Plasma samples from control ($n = 48$) and emphysema patients ($n = 60$) were used to measure C1q concentration using ELISA. Box, median and interquartile range; whiskers, min to max range. $^{***}P < 0.001$. (**F**) Human CD1a⁺ lung cells isolated by autoMACS were cultured in complete medium (RPMI-1640 with 10% FBS and Pen-Strep) at a concentration of 1×10^6/mL and treated with increasing concentration of purified human IL-1β (100 pg/mL, 1 ng/mL) for 48 hours or with medium alone as the vehicle. The expression level of *C1QA* was measured by quantitative reverse transcription PCR (qPCR). (Normalized to *18S* expression). $n = 3$; $^{*}P < 0.05$. Results are represented as mean ± SEM, from 3 independent experiments. (**G**) Knockdown of C1QA expression in human cDCs was achieved by transfection of C1QA-specific siRNA. Scrambled siRNA was transfected as a control. The expression of *C1QA* mRNA was measured by qPCR (Normalized to 18S expression). $^{***}P < 0.001$. (**H** and **I**) CD4⁺ T cells isolated from PBMCs were cocultured with allogeneic APCs shown in 10:1 ratio (CD4⁺ T cells and APCs) for 3 days, and CD25⁺Foxp3⁺ (**H**) and CD25⁺Foxp3⁻ (**I**) T cell population were measured using flow cytometry. $^{***}P < 0.001$. (**J**) The concentration of IL-17A in the supernatant from cell cultures in (**I**) was measured by multiplex assay. $^{***}P < 0.001$. *P* values were determined by the Mann-Whitney nonparametric test.

C1q plasma level (Figure 1E), and airflow obstruction based on the global initiative for obstructive lung disease (GOLD) criteria (37) revealed a significant reduction in serum C1q concentration in patients with more advanced disease (stages III and IV; Supplemental Figure 2D). Together, these findings support the idea that the pathophysiological changes in smokers with emphysema are linked to a reduced expression of C1q in this COPD endotype.

C1q deficiency in human APCs skews Treg and Th17 cell induction. We and others have previously shown that the NLRP3 inflammasome and associated cytokines are required for the inflammation induced by nano-sized carbon black particle inhalation (3). Therefore, we next examined whether activation of the NLRP3 inflammasome could play a direct role in the loss of C1q expression in APCs. We found that IL-1β, a proinflammatory cytokine that is released in response to inflammasome activation (38), dose-dependently inhibited C1q expression in lung CD1a⁺ cells, suggesting their potential link (Figure 1F). In addition to the pathogenic role of Th17 cells in the progression of emphysema, Tregs also play a critical role in induction of chronic inflammation (39–41). To determine whether C1q plays a role in Treg and Th17 cell induction, we used siRNA to knockdown C1q in human monocyte-derived APCs. *C1QA*-specific siRNA significantly reduced its mRNA expression in APCs, and when cocultured with naive CD4⁺ T cells, they decreased the frequency of CD25⁺Foxp3⁺ Treg cells, increased the frequency of CD25⁺Foxp3⁻ activated T cells, and enhanced secretion of IL-17A compared with control transfected cells (Figure 1, G–J).

To determine whether our findings in humans are consistent with the smoke-induced animal model of emphysema, we exposed mice to chronic smoke (Figure 2A). Emphysema developed in mice and the mice showed increased inflammatory cells in the bronchoalveolar lavage (BAL) fluid, the composition of which was greater than 90% macrophages (Figure 2, B and C). Consistent with the findings in smokers with emphysema, we found that *C1q* expression is also significantly reduced in BAL inflammatory cells isolated from chronic smoke–exposed mice compared with air control (Figure 2D). Using an in vitro coculture assay, we also found that APCs from mice with global knockout of C1q (*C1q*$^{-/-}$ mice) reduce Foxp3⁺

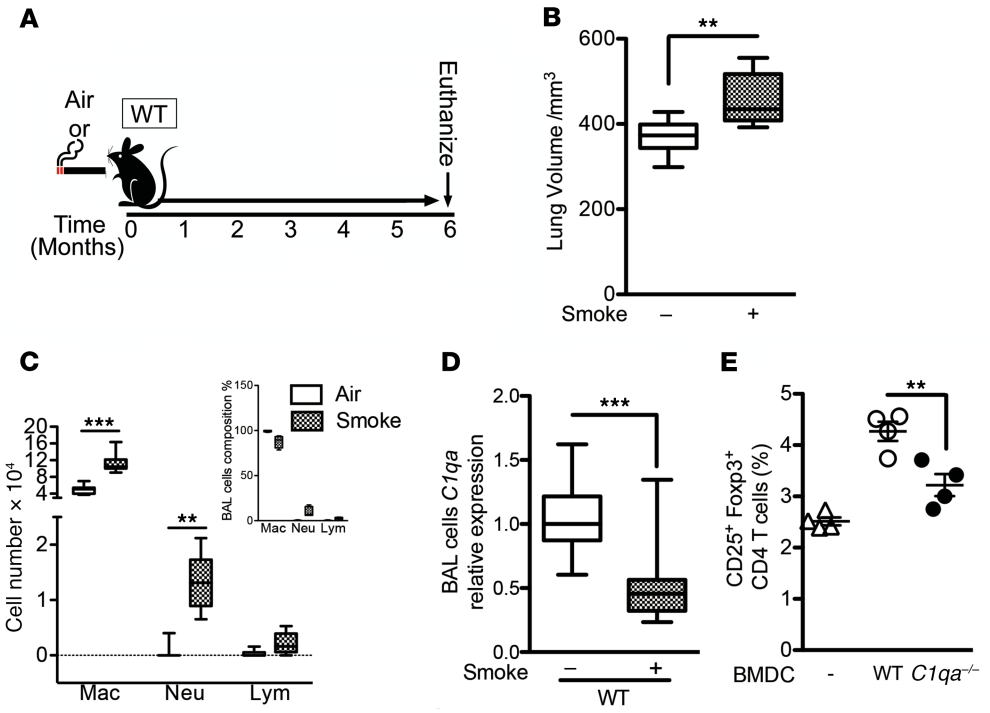

Figure 2. Cigarette smoke inhibits C1q expression in APCs and increases Th17 cells. (**A**) Schematic diagram showing 4-month smoke, or air exposure using C57BL/6J (WT) mice. (**B**) Micro-CT analysis of lung volume from WT mice exposed to air or cigarette smoke for 4 months (n = 9 each). Box, median and interquartile range; whiskers, min to max range. (**C**) BAL cell differential shows increased macrophages and neutrophils in smoke-exposed mice; inset shows percentage composition of BAL cells in air- and smoke-exposed mice (n = 15 each). Box, median and interquartile range; whiskers, min to max range. (**D**) Expression of *C1q* mRNA in BAL cells isolated from mice exposed to 6 months of air or cigarette smoke was measured by qPCR and normalized to *18S* expression. n = 24 in the air and n = 23 in the smoke group; $^{***}P < 0.001$, as determined by the Student's t test. Box, median and interquartile range; whiskers, min to max range. (**E**) $CD4^+$ splenic T cells isolated from naive WT mice were cocultured with APCs from WT or *C1qa*$^{-/-}$ mice at a 10:1 ratio ($CD4^+$ T cells and APCs) for 3 days, and the population of $Foxp3^+$ T cells were measured by flow cytometry. $^{**}P < 0.01$ (n = 4). Results are represented as mean ± SEM, from 3 independent experiments. P values were determined by a 1-way ANOVA test with Bonferroni's correction for multiple comparisons.

expression in congenic $CD4^+$ T cells compared with APCs isolated from C1q-sufficient WT mice (Figure 2E). Together, our findings in humans and mice indicate that cigarette smoke–mediated downregulation of C1q in APCs results in a reduction of Treg induction and induces activation of $CD4^+$ T cells that are pathophysiologically similar to human emphysema (12).

C1q potentiation of Tregs and inhibition of Th17 cells. Our findings thus far indicated that C1q is downregulated in smokers with emphysema and in mice exposed to chronic smoke; we also found that reduction of C1q expression in APCs promotes Th17 cell induction. We next investigated whether C1q can enhance T helper cell differentiation in vitro. We found that in the presence of C1q, naive $CD4^+$ T cells stimulated under Treg-skewing conditions (42), significantly increased $Foxp3^+$ in $CD25^+$ cells in vitro (Figure 3, A and B). Increased *Foxp3* mRNA expression seen under the same Treg-skewing conditions further confirmed the potentiation effect of C1q in $CD4^+$ T cells (Figure 3C). TGF-β also reduced PD-1 expression, although in the presence of C1q, PD-1 expression was maintained at similar levels compared with control conditions (Supplemental Figure 3A). The effect of C1q on Treg potentiation was dependent on Treg-skewing conditions because $CD4^+$ T cells treated with C1q alone failed to show enhanced Treg differentiation (Figure 3B). In addition, in the presence of C1q and under Treg differentiation conditions, human $CD4^+$ T cells showed increased Treg differentiation in vitro (Supplemental Figure 3B). In contrast, under Th17-skewing conditions, the addition of C1q to naive $CD4^+$ T cells resulted in a significant reduction in IL-17A expression compared with control cells (Figure 3, D and E). Consistently, we found significant suppression of $ROR\gamma T^+$ T cells in response to C1q treatment (Figure 3F).

C1q induces Treg differentiation in vivo. The studies thus far suggested that under Treg-skewing conditions, C1q promotes Tregs and under Th17-skewing conditions, C1q inhibits Th17 differentiation in vitro.

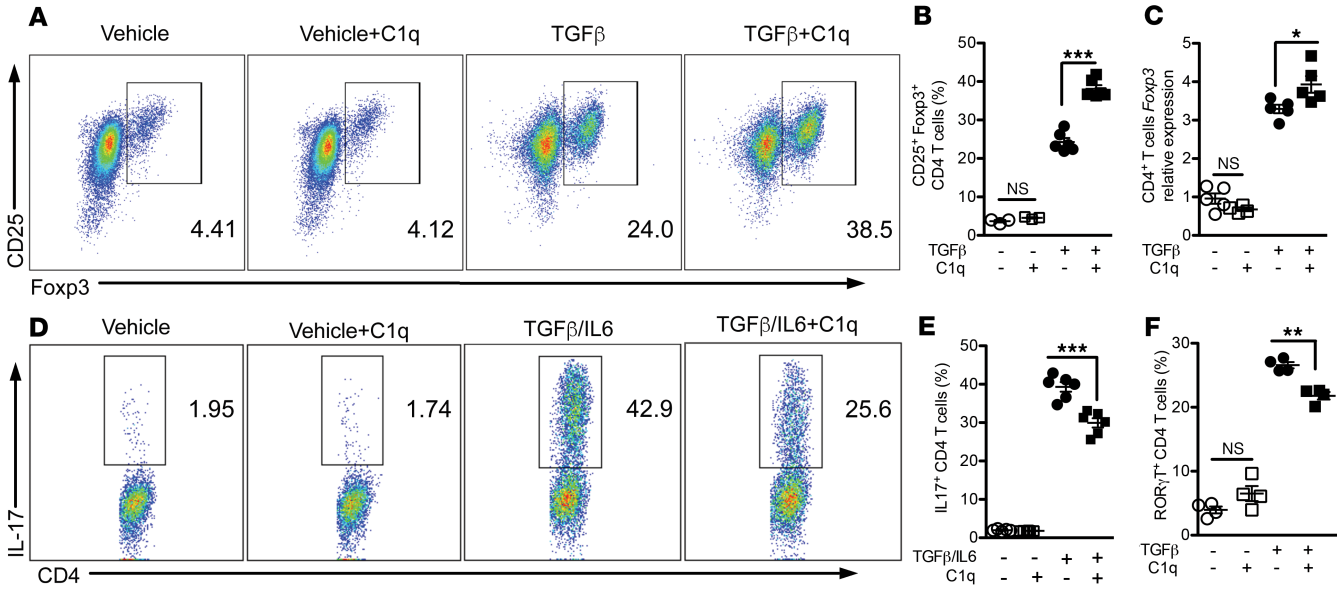

Figure 3. C1q enhances Tregs while it inhibits Th17 cell differentiation in vitro. Mouse CD4⁺ T cells were isolated from splenocytes by autoMACS. (**A**) Representative flow plot of CD4⁺ T cells isolated from the spleen and stimulated with anti-CD3/anti-CD28; cells were differentiated under Treg condition (TGF-β, anti–IL-4, anti–IFN-γ) with or without C1q for 3 days; CD4⁺ T cells in vehicle control condition were stimulated with anti-CD3/anti-CD28 but received PBS for 3 days. Tregs in culture were identified by flow cytometry using CD25 and Foxp3 markers. (**B**) Cumulative data shown in **A** were summarized (n = 3 for control and C1q; n = 6 for TGF-β and TGF-β + C1q). Results are represented as mean ± SEM, from 3 independent experiments. (**C**) Expression of Foxp3 mRNA in culture described in **A** was measured by qPCR (n = 5 in each group, normalized to *18S* expression). Results are represented as mean ± SEM, from 3 independent experiments. (**D**) Representative CD4⁺ T cells differentiated under Th17 condition (e.g., IL-6, TGF-β, anti–IL-4, anti–IFN-γ) for 3 days. IL-17 production was measured using intracytoplasmic cytokine staining. (**E**) Cumulative data shown in (**D**) is summarized (n = 6 for control and C1q; n = 6 for TGF-β and TGF-β + C1q). (**F**) CD4⁺ T cells expressing RoRγt in culture described in **D** were measured by qPCR (n = 4 in each group, normalized to *18S* expression). Results are represented as mean ± SEM, from 3 independent experiments. *P < 0.05, **P < 0.01, ***P < 0.001; P values were determined by 1-way ANOVA test with Bonferroni's correction for multiple comparisons.

To examine the physiological effects of C1q, we next examined whether it alters lung immune cell profiles in vivo. Naive mice given intranasal C1q showed no increase in BAL fluid cellularity or inflammation-associated genes, including MMPs, compared with control mice (Figure 4, A and B, and Supplemental Figure 4, A and B), indicating that intranasal C1q treatment does not induce lung inflammation. In contrast, mice treated with C1q showed an increase in the relative abundance of CD25⁺Foxp3⁺ Tregs compared with vehicle-treated mice (Figure 4C). We found no significant differences in the number of lung Th17 cells or APCs after intranasal C1q treatment (Supplemental Figure 4, C and D). Notably, both IL-10 and TGF-β concentrations were also increased in the lung homogenates derived from C1q-treated mice, demonstrating that it promotes the production of immune regulatory cytokines (Figure 4, D and E). Consistent with our in vitro findings, the mRNA analyses of BAL cells showed significant increases in *Foxp3* expression and several markers of tolerogenic cDCs (e.g., CD103 and PDL1) in the C1q-treated group compared with vehicle control (Figure 4, F–H). Together, these findings indicate that C1q may promote the development of lung immune tolerance.

Aberrant T cell activation in C1qa-deficient mice. We next tested the role of C1q in T cell homeostasis by measuring the relative abundance of CD4⁺ and CD8⁺ T cell subsets in the spleen, mesenteric, and lung-draining lymph nodes from *C1qa*$^{-/-}$ and WT littermate mice. Compared with WT littermate mice, 12-month-old *C1qa*$^{-/-}$ mice showed lower relative expression of CD62L in CD4⁺ and CD8⁺ T cells and higher relative expression of CD44^{hi} activated CD4⁺ and CD8⁺ T cells, indicating an overall increase in activation of lymphocytes under steady state (Figure 5, A–D). In addition, *C1qa*$^{-/-}$ mice had significantly reduced splenic Tregs (Foxp3⁺CD25⁺ T cells; Figure 5E), which also showed decreased expression of CD62L and inducible T cell costimulator (ICOS; Figure 5, F–I). Consistent with the natural increase in activation markers in T cells from 12-month-old *C1qa*$^{-/-}$ mice, we found increased relative abundance of CD62L^{lo} CD4⁺ and CD8⁺ splenic T cells derived from 5-month-old *C1qa*$^{-/-}$ mice (Supplemental Figure 5). Together, our findings suggest that global loss of C1q results in systemic immune dysregulation that manifests as increased T cell activation and aberrant Treg phenotypes in peripheral lymphoid organs.

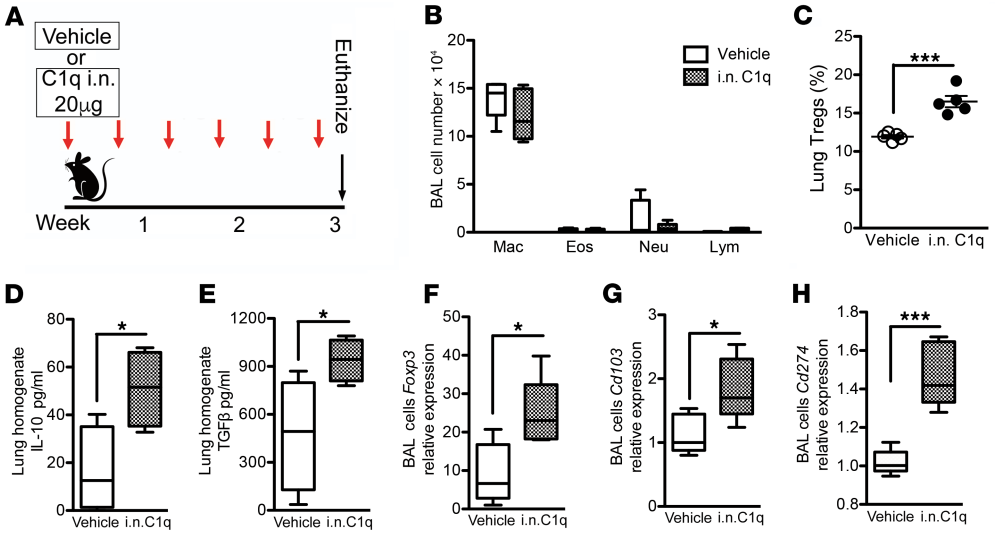

Figure 4. Intranasal C1q induces Tregs in lungs of WT mice. Eight-week-old WT (C57BL/6J) mice were treated with intranasal (i.n.) C1q (20 μg, twice per week) for 3 weeks. (**A**) Schematic representation of C1q treatment in naive mice. (**B**) Bronchoalveolar lavage (BAL) fluid analyses from the C1q-treated or vehicle-treated mice showing a similar number of macrophages (Mac), eosinophil (Eos) lymphocytes (Lym), and neutrophils (Neu). $n = 5$ in each group. Box, median and interquartile range; whiskers: min to max range. (**C**) Cumulative flow cytometry analysis showed the population of $CD25^+Foxp3^+$ CD4 T cells in lungs of the same group of mice. $^{***}P < 0.001$, as determined by the Student's t test. $n = 5$ in each group. Results are represented as mean ± SEM, from 2 independent experiments. Concentrations of IL-10 (**D**) and TGF-β (**E**) in lung homogenate were measured by ELISA. $^*P < 0.05$, as determined by the Student's t test. $n = 5$ in each group. Results are represented as mean ± SEM, from 2 independent experiments. Expression of *Foxp3* (**F**), *Cd103* (**G**), and *Cd274* (PD-L1) (**H**) in BAL cells was measured using quantitative reverse transcription PCR (qPCR). $n = 5$ in each group. Results are represented as mean ± SEM, from 2 independent experiments. $^*P < 0.05$, $^{***}P < 0.001$, as determined by the Student's t test.

$C1qa^{-/-}$ mice show excessive cigarette smoke–induced emphysema. We next tested the effect of *C1q* deficiency in response to chronic cigarette smoke exposure. *$C1qa^{-/-}$* mice exposed to 4 months of cigarette smoke (Figure 6A) showed increased lung mononuclear cell infiltration in the H&E staining of lung tissue compared with age-matched WT littermate mice exposed to smoke (Figure 6B). Similarly, we found significantly increased macrophages and neutrophils in the BAL fluid isolated from *$C1qa^{-/-}$* compared with WT littermate mice (Figure 6C). Consistent with increased inflammation, we found that *Foxp3* expression and the relative abundance of $Foxp3^+CD25^+$ Tregs were significantly decreased in the BAL fluid cells and in the lung cells isolated from *$C1qa^{-/-}$* mice exposed to cigarette smoke compared with WT littermate mice (Figure 6, D and E). *$C1qa^{-/-}$* mice exposed to smoke also showed an increased recruitment of APCs marked by high expression of MHC-II, CD11b, and CD11c into the lungs (Figure 6F) as well as an increased relative abundance of Th17 cells (Figure 6G). Together, these findings indicate that the absence of *C1q* exacerbates the production of lung Th17 cells following exposure to cigarette smoke.

Exogenous C1q attenuates cigarette smoke–induced emphysema. We next tested whether restoring C1q in the lungs could attenuate cigarette smoke–mediated lung inflammation and emphysema in mice. WT mice were exposed to 4.5 months of smoke, after which they were treated either intranasally with C1q or vehicle control (PBS), twice weekly and were exposed to an additional 1.5 months of smoke (Figure 7A). Micro CT quantification of lung volumes showed that emphysema was reduced in smoke-exposed mice treated with C1q compared with the vehicle group (Figure 7B). Lung histology and unbiased quantitative morphometry of the same mice confirmed reduced lung destruction in the C1q-treated mice as measured by mean linear intercept (MLI; Figure 7, C and D). Consistently, BAL fluid cellularity showed reduced neutrophils, and the whole lung showed reduced Th17 cells in C1q-treated mice that were exposed to cigarette smoke (Figure 7, E and F). However, C1q treatment did not alter the recruitment of APCs marked by high expression of MHC-II, CD11b, and CD11c to the lungs of mice exposed to cigarette smoke (Figure 7G).

Notably, IL-6 and IL-1β expression, two proinflammatory cytokines that are critical in emphysema development, were significantly reduced in BAL fluid cells isolated from smoke-exposed but C1q-treated mice (Figure 8, A and B). We have shown that cigarette smoke reduces the expression of *Pparg*, a critical antiinflammatory transcription factor, in lung APCs (36). We found that C1q treatment restored *Pparg* expression in BAL

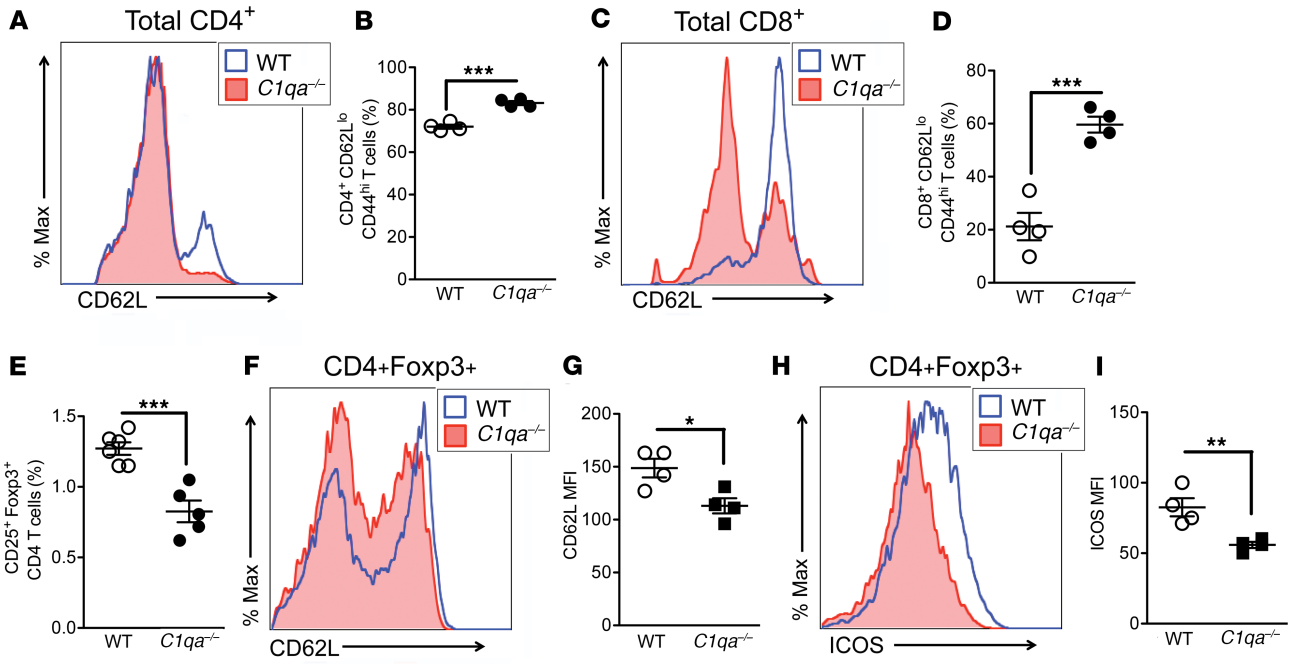

Figure 5. Increased T cell activation in *C1qa*$^{-/-}$ mice. Total splenocytes were isolated from 12-month-old WT or *C1qa*$^{-/-}$ mice. Representative histograms and summarized mean fluorescence intensity of CD62L on CD4$^+$ (**A** and **B**) and CD8$^+$ (**C** and **D**) T cells as measured by flow cytometry. $n = 4$ in each group. Results are represented as mean ± SEM, from 2 independent experiments. ***$P < 0.001$ was determined by Student's t test. (**E**) Relative abundance of CD25$^+$Foxp3$^+$ CD4$^+$ T cell population in the spleen was measured by flow cytometry. $n = 6$ in WT and $n = 5$ in *C1qa*$^{-/-}$ group. Results are represented as mean ± SEM, from 2 independent experiments. ***$P < 0.001$ was determined by Student's t test. Representative histogram and summarized the mean fluorescent intensity of CD62L (**F** and **G**) and ICOS (**H** and **I**) on CD4$^+$ Foxp3$^+$ T cells in the spleen. $n = 4$ in each group. Results are represented as mean ± SEM, from 2 independent experiments. **$P < 0.01$ was determined by Student's t test.

fluid cells, implicating a potential mechanism of C1q-mediated immune regulation (Figure 8C). Consistent with the induction of immune tolerance, *Foxp3* and *Il10* expression and the relative abundance of Tregs were all significantly increased in the lung of C1q-treated mice exposed to cigarette smoke (Figure 8, D–F). These data suggest that exogenous C1q inhibits smoke-induced lung inflammation and can prevent emphysema development in mice exposed to smoke. Together these findings indicate that C1q attenuates pulmonary inflammation induced by chronic cigarette smoke exposure via acting on both APCs and CD4$^+$ T cells. The effect of C1q in the induction of immune tolerance was specific because intranasal human serum albumin showed no significant reduction of inflammatory cell infiltration to the lung in the same protocol (Supplemental Figure 6).

C1q-induced Treg cell potentiation is caused by cell cycle modulation. To investigate the mechanism of C1q-induced Treg potentiation, we performed unbiased RNA-Seq screening and pathway analysis during an early time point using human CD4$^+$ T cells stimulated with TGF-β with or without C1q (Supplemental Figure 7). Among multiple pathways, we found that the addition of C1q significantly alters genes related to interleukin signaling and cell cycle pathways (Figure 9, A–D). C1q has also been shown to block the proliferation of human fibroblasts via suppression of DNA synthesis and arrest in the G1 phase (43); therefore, we next examined whether C1q also affects T cell proliferation under Th1, Th17, or Treg polarizing conditions. We found no significant effect of C1q on Th1 differentiation conditions (Supplemental Figure 8A); however, although TGF-β inhibited proliferation of Foxp3$^-$ CD4$^+$ T cells, in the presence of C1q, this inhibition was significantly potentiated (Figure 9, E and F). In response to Th17 differentiation conditions, IL-6/TGF-β did not alter RORγT$^+$CD4$^+$ Th17 cell proliferation; however, in the presence of C1q, it was significantly downregulated (Figure 9, G and H). In addition, the function of C1q in cell apoptosis has been shown by several studies. C1q can induce apoptosis in multiple tumor cells, including ovarian cancer and prostate cancer cell lines (44, 45). However, we did not find that C1q altered apoptosis in T cells during Treg or Th17 differentiation (Supplemental Figure 8B). Together, these findings suggest that the local presence of C1q selectively enhances Treg cell differentiation and proliferation, while it inhibits CD4$^+$ Foxp3$^-$ and RORγt$^+$ T cells under Treg and Th17 cell differentiation conditions, respectively.

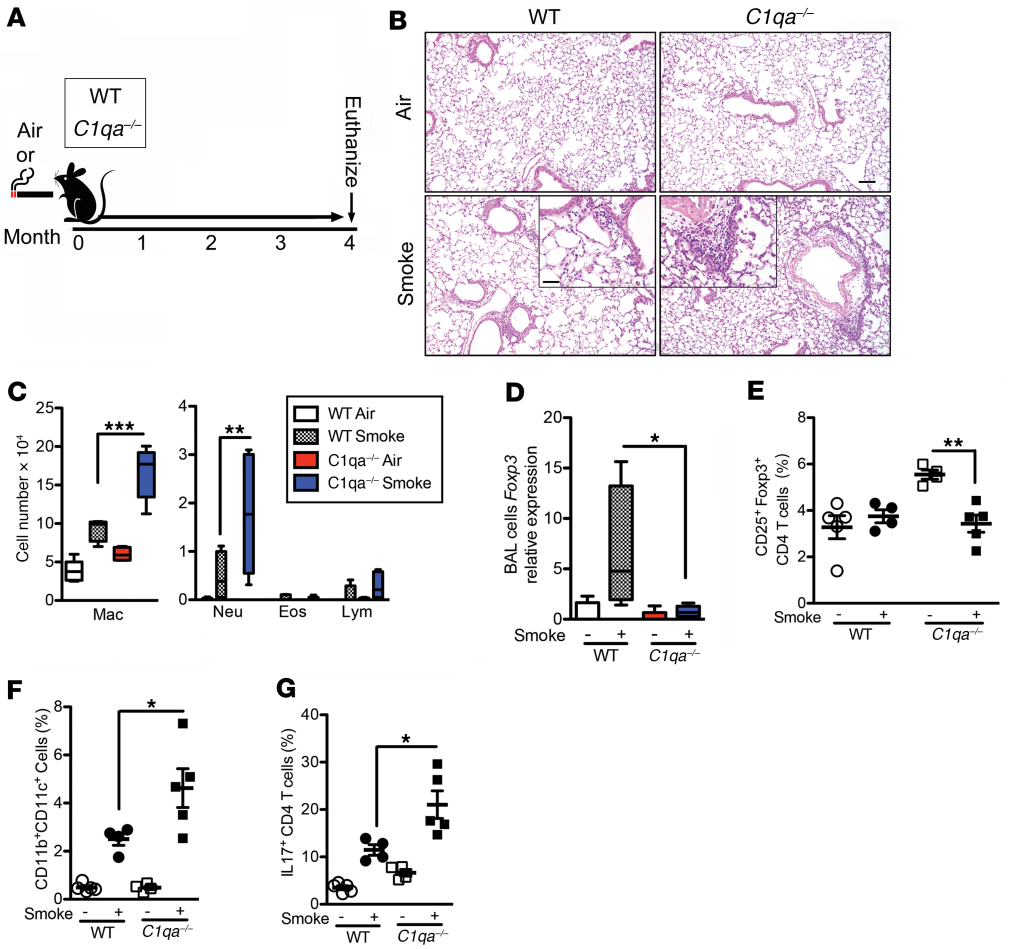

Figure 6. C1q deficiency results in exaggerated smoke-induced emphysema. WT mice and *C1qa*$^{-/-}$ mice were exposed to cigarette smoke or air for 4 months. (**A**) Schematic diagram of experimental design. (**B**) Representative images of H&E-stained lung sections from air-exposed or smoke-exposed WT and *C1qa*$^{-/-}$ mice. Scale bar: 100 μm (25 μm in inset). (**C**) Bronchoalveolar lavage (BAL) fluid analyses from the same group of mice showing macrophages (Mac), neutrophils (Neu), eosinophil (Eos), and lymphocytes (Lym). n = 5 in WT Air; n = 4 in *C1qa*$^{-/-}$ Air; n = 4 in WT Smoke; n = 5 in *C1qa*$^{-/-}$ Smoke. Box, median and interquartile range; whiskers, min to max range. $^{**}P < 0.01$, $^{***}P < 0.001$, as determined by 1-way ANOVA with Bonferroni's correction for multiple comparisons. (**D**) Expression of *Foxp3* mRNA in BAL cells was measured by quantitative reverse transcription PCR (qPCR). n = 5 in WT Air; n = 4 in *C1qa*$^{-/-}$ Air; n = 4 in WT Smoke; n = 5 in *C1qa*$^{-/-}$ Smoke. Box, median and interquartile range; whiskers, min to max range. Results are represented as mean ± SEM, from 2 independent experiments. $^{*}P < 0.05$, as determined by the 1-way ANOVA with Bonferroni's correction for multiple comparisons. (**E**) Cumulative flow cytometry analysis showed the population of CD25^{+}Foxp3^{+} CD4^{+} T cells in lungs of the same group of mice. n = 5 in WT Air; n = 4 in *C1qa*$^{-/-}$ Air; n = 4 in WT Smoke; n = 5 in *C1qa*$^{-/-}$ Smoke. Results are represented as mean ± SEM, from 2 independent experiments. $^{*}P < 0.05$, was determined by the 1-way ANOVA with Bonferroni's correction for multiple comparisons. (**F**) Cumulative relative abundance of CD11b^{+}CD11c^{+} lung APCs in the same experiment. n = 5 in WT Air; n = 4 in *C1qa*$^{-/-}$ Air; n = 4 in WT Smoke; n = 5 in *C1qa*$^{-/-}$ Smoke. Results are represented as mean ± SEM, from 2 independent experiments. $^{*}P < 0.05$, was determined by 1-way ANOVA with Bonferroni's correction for multiple comparisons. (**G**) Cumulative intracellular cytokine staining of IL-17A in CD3^{+}/CD4^{+} T cell population. n = 5 in WT Air; n = 4 in *C1qa*$^{-/-}$ Air; n = 4 in WT Smoke; n = 5 in *C1qa*$^{-/-}$ Smoke. Results are represented as mean ± SEM, from 2 independent experiments. $^{*}P < 0.05$, as determined by the 1-way ANOVA with Bonferroni's correction for multiple comparisons.

Discussion

In this report, we show that C1q produced by APCs is a critical mediator in Treg and Th17 cell differentiation in cigarette smoke–induced lung inflammation. Multiple factors could contribute to the dysregulation of C1q in innate immune cells. However, we show that proinflammatory cytokines induced by cigarette smoke (e.g., IL-1β) inhibit the expression of C1q; reduction of C1q reduced Treg cell induction and increased Th17 cells that promote autoimmunity. C1q deficiency exaggerated Th17 cell responses and induced aberrant T cell activation in the peripheral lymphoid organs of smoke-exposed mice.

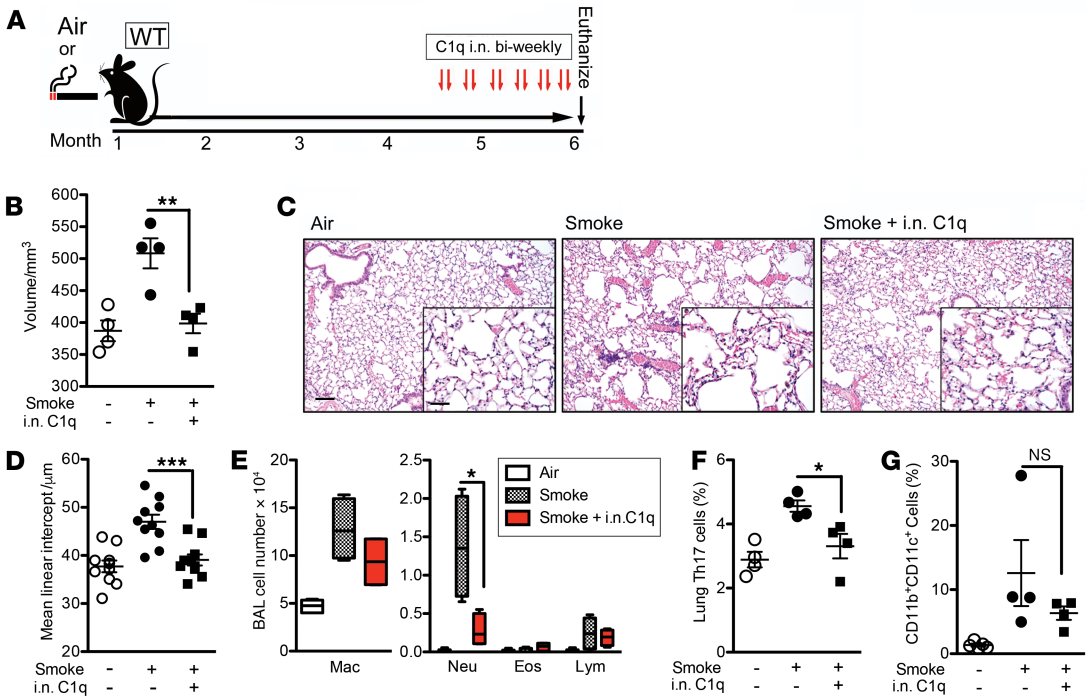

Figure 7. Intranasal C1q attenuates cigarette smoke–induced emphysema. WT mice were exposed to cigarette smoke or air for 6 months. Intranasal (i.n.) C1q was given to smoke-exposed mice (20 μg, twice per week) for a total of 6 weeks before termination of the experiment at 6 months. (**A**) Schematic representation of experimental design. (**B**) Micro-CT quantification of lung volume and (**C**) representative images of H&E-stained lung sections from air-exposed, smoke-exposed, and smoke-exposed mice treated with C1q. Scale bar: 100 μm (25 μm in inset). $n = 4$ in each group. Results are represented as mean ± SEM, from 3 independent experiments. $^{**}P < 0.01$, was determined by 1-way ANOVA with Bonferroni's correction for multiple comparisons. (**D**) Mean linear intercept using unbiased morphometry in the indicated groups of mice described in (**A**). $n = 10$ in each group. Results are represented as mean ± SEM, from 3 independent experiments. $^{***}P < 0.001$, was determined by the 1-way ANOVA with Bonferroni's correction for multiple comparisons. (**E**) Bronchoalveolar lavage (BAL) fluid analyses from the same group of mice showing macrophages (Mac), neutrophils (Neu), eosinophil (Eos), and lymphocytes (Lym). $n = 4$ in each group. Box, median and interquartile range; whiskers, min to max range. $^{*}P < 0.05$, was determined by 1-way ANOVA with Bonferroni's correction for multiple comparisons. Representative of 3 independent experiments. (**F**) Cumulative intracellular cytokine staining of IL-17A in $CD3^+/CD4^+$ T cells. $n = 4$ in each group. Results are presented as mean ± SEM; representative of 3 independent experiments. $^{*}P < 0.05$, was determined by the 1-way ANOVA with Bonferroni's correction for multiple comparisons. (**G**) Cumulative relative abundance of $CD11b^+CD11c^+$ lung APCs in the same experiment. $n = 4$ in each group. Results are represented as mean ± SEM, from 3 independent experiments.

Conversely, exogenous C1q treatment in vitro and in vivo induced Treg cells and reduced Th17 cells in association with dampened inflammatory responses. Together, these findings reveal the previously unknown and critical role of C1q as a regulator of immune responses in response to cigarette smoke–mediated inflammation and suggest a new strategy to treat emphysema and potentially other autoinflammatory diseases.

Previous studies have shown that APCs isolated from *C1q*$^{-/-}$ mice express a higher level of IL12p40 in response to lipopolysaccharide and promote the induction of Th1 and Th17 cells (35). We provide evidence that under normal conditions, C1q deficiency results in aberrant T cell activation and altered Treg cell phenotype as mice age, but this autoinflammatory condition is exaggerated when mice are exposed to cigarette smoke. Whereas the onset of autoimmunity in *C1q*$^{-/-}$ mice is highly age dependent, we found early evidence for aberrant T cell activation, albeit milder, in 5-month-old mice. Short-term intraperitoneal injection of C1q in a model of allergic airway diseases failed to show a significant expansion of Treg cells in blood, the lungs, and the spleen (46). These findings are in contrast with chronic and lung-specific (e.g., intratracheal) administration of C1q results in potent upregulation of Tregs and decreased inflammation in the airways, suggesting localized induction of Tregs that control inflammation.

C1q, as one of the initiating components of the classical complement pathway, also functions through complement-independent pathways to control and regulate both innate and acquired immunity (47). In support of this concept, several studies have shown a critical role for C1q in the phagocytic uptake of apoptotic cells by macrophages, a task that is crucial to prevent unnecessary inflammation caused by dying cells (48). In addition, several receptors, including CD91, calreticulin, and Scarf1, have been identified to bind C1q and facilitate the clearance of C1q-coated apoptotic cells (49–51). However, our findings here provide what we believe is a new function for C1q in mechanisms related to activation of autoimmunity.

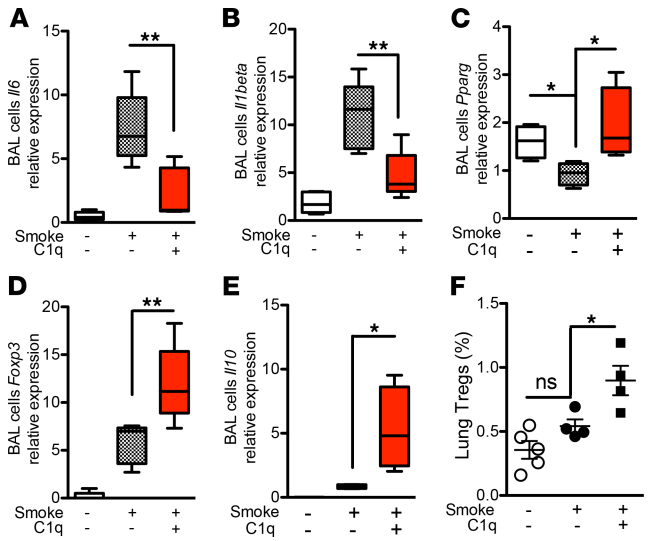

Figure 8. Intranasal C1q decreases cigarette smoke–induced inflammatory cytokine and enhances Treg-related genes. Expression of *Il6* (**A**) and *Il1beta* (**B**) mRNA in BAL cells were measured by quantitative reverse transcription PCR (qPCR) in experimental conditions described in Figure 7 (normalized to *18S*). $n = 5$ in each group. Box, median and interquartile range; whiskers, min to max range. $^{**}P < 0.01$, as determined by 1-way ANOVA with Bonferroni's correction for multiple comparisons. Representative of 3 independent experiments. (**C**–**E**) Expression of *Pparg* (**C**) *Foxp3* (**D**) and *Il10* (**E**) mRNA in BAL cells was measured by quantitative reverse transcription PCR (qPCR, normalized to *18S*). $n = 5$ in each group. Box, median and interquartile range; whiskers, min to max range. $^{*}P < 0.05$, $^{**}P < 0.01$, as determined by 1-way ANOVA with Bonferroni's correction for multiple comparisons. Representative of 3 independent experiments. (**F**) Cumulative data show relative abundance of $CD25^{+}Foxp3^{+}$ $CD4^{+}$ T cells in the lungs of the same group of mice using flow cytometry. $n = 5$ in Air group; $n = 4$ in Smoke and Smoke + C1q group. Results are represented as mean ± SEM; representative of 3 independent experiments. $^{*}P < 0.05$, as determined by 1-way ANOVA with Bonferroni's correction for multiple comparisons.

C1q has previously been shown to regulate tolerogenic immune responses by influencing the differentiation and polarization of non–T cells (52, 53). For example, C1q can reduce the production of proinflammatory cytokines expressed by macrophages and cDCs and reduce their capacity to induce Th1/Th17 cell responses (53). Moreover, LAIR-1 has been identified to be an inhibitory receptor for C1q on monocytes and binding of LAIR-1 to C1q limited the production of proinflammatory cytokines (54). Complementing these findings, our studies now show that C1q can dampen Th17 cell responses and promote Tregs in mice exposed to chronic smoke. To address the mechanism for the role of C1q in acquired immunity, we found that C1q does not directly change Treg differentiation responses in vitro, although in combination with TGF-β, it enhances Foxp3 expression. Using RNA-Seq and pathway analysis, we identified enhancement of cytokine signaling and cell cycle pathways in $CD4^{+}$ T cells that were stimulated with TGF-β and C1q. Notably, we found that C1q inhibited proliferation of $Foxp3^{-}$ and $RoR\gamma t^{+}$ $CD4^{+}$ T cells, indicating selective inhibition of these cell populations as a potential mechanism for enhancement of Treg population in the presence of TGF-β. Our findings thus further reveal the complex role that C1q plays in immune regulation.

C1q deficiency resulting from genetic defects or the production of neutralizing autoantibodies is strongly linked to the development of SLE (55). In patients with genetically based *C1Q* deficiency, approximately 90% develop SLE, and autoimmune-mediated SLE-like nephritis develops in $C1q^{-/-}$ mice after 8 months of age (33). The link between C1q deficiency and the development of SLE could be explained partially by several mechanisms, including the defective apoptotic cell clearance, aberrant autoreactive B cells, and lack of tolerogenic cDCs (27). However, our comprehensive evaluation of the immune cell profiles in $C1q^{-/-}$ mice indicates that C1q can mediate suppression of proinflammatory T cells that could lead to organ-specific autoinflammation (e.g., SLE).

Based on our findings, we propose that C1q may play similar roles in the development of emphysema. Several clinical studies have documented that a subset of former smokers shows a rapid decline in their lung function, even long after smoking cessation (56, 57). These and other observations indicate that such decline is linked to rapidly progressive emphysema that occurs in the context of pathogenic

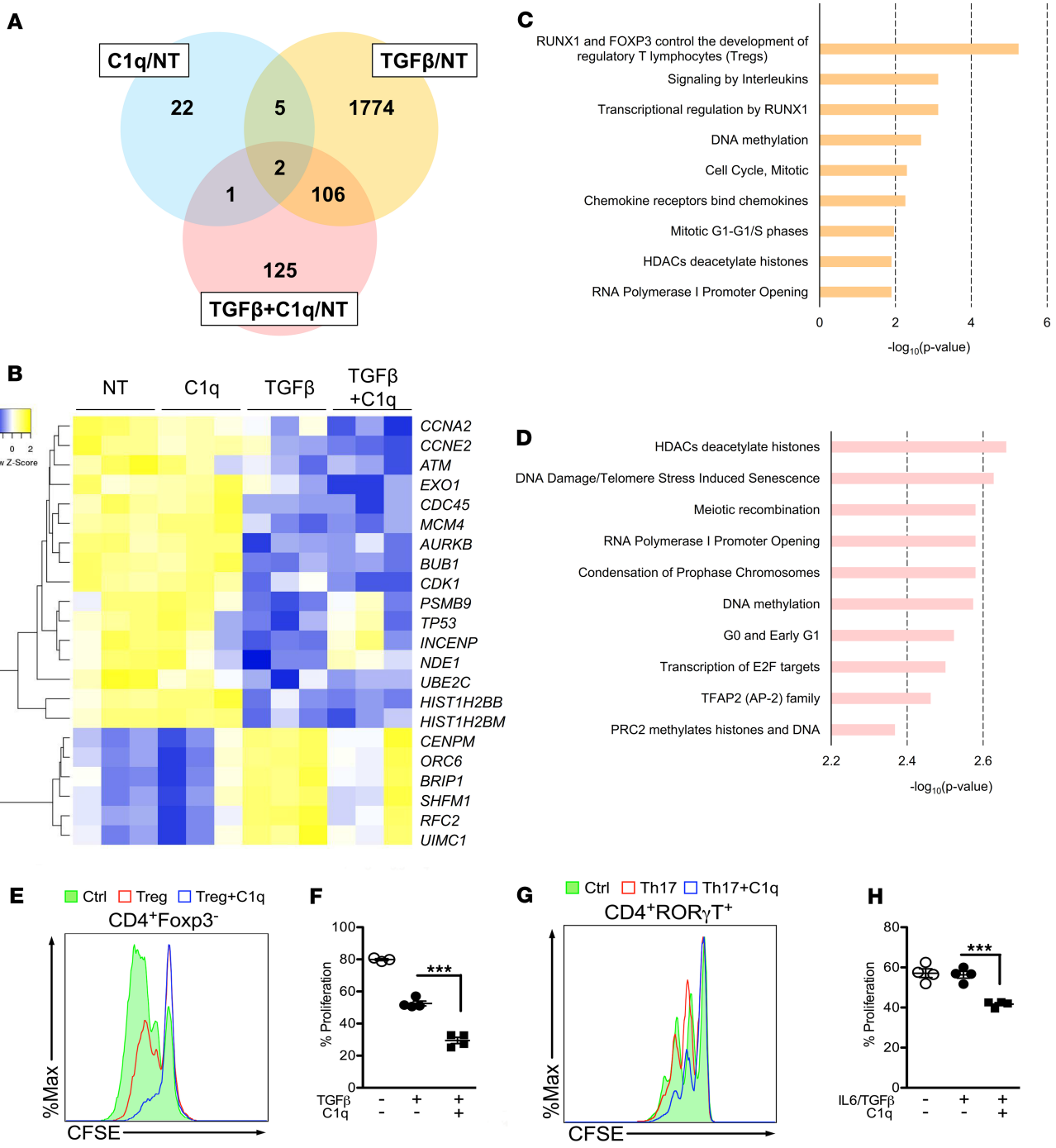

Figure 9. RNA-Seq and pathway analysis of C1q-treated CD4⁺ T cells. Human CD4⁺ T cells were isolated from PBMCs and cultured with vehicle (no treatment; NT), C1q, TGF-β with or without C1q for 48 hours. Total RNA was isolated from the cells and analyzed by RNA-Seq using standard protocols. (**A**) Venn diagram was constructed to show the number of significant unique or shared gene changes between the 3 treatment conditions: C1q, TGF-β, and C1q + TGF-β. The number of transcripts that met the cutoff (adjusted *P* value < 0.01; fold change > 1.4 upregulated/downregulated) for each treatment are shown in each circle. (**B**) Unsupervised RNA-Seq expression profile of 22 cell cycle regulatory genes. Heatmap of cell cycle–related differentially expressed transcripts between C1q, TGF-β, and C1q + TGF-β groups. Row *Z*-score is shown in the upper left area. Color keys on the top show lower relative expression as blue and higher relative expression as yellow. Pathway analysis, using the Reactome bioinformatics tool, identified major signaling pathways that showed significance; (**C**) 106 overlapped genes in TGF-β and TGF-β + C1q treatment group; (**D**) 125 genes in the TGF-β + C1q group were used for pathway analysis. Protein-coding genes were selected for pathway analyses. (**E**–**H**) Mouse splenic CD4⁺ T cells were labeled with CFSE and then differentiated under Treg or Th17 (IL-6/TGF-β) conditions in the presence or absence of C1q. After stimulation, CD4⁺Foxp3⁻ cells (**E** and **F**) and CD4⁺RORγT⁺ cells (**G** and **H**) were gated and the fluorescent intensity of CFSE was plotted and percentage proliferation was summarized based on CFSE dilution. $n = 3$ in Naive; $n = 4$ in TGF-β and TGF-β + C1q in (**F**). $n = 4$ in each group in (**H**). Results are presented as mean ± SEM, from 3 independent experiments. $^{**}P < 0.01$, $^{***}P < 0.001$ as determined by 1-way ANOVA with Bonferroni's correction for multiple comparisons.

Th1 and Th17 cell activation that is detectable in both the peripheral lung and blood (9, 10). Because most of our patients were recruited from the VA medical center, the distribution of men is different between the groups, and our control subjects were younger. However, based on our prior data, the inflammation markers are not different between men and women smokers, indicating that despite this caveat, our findings represent disease-related differences. In addition, our confirmatory studies, using age-matched female mice, also showed the same reduction in C1q and Treg responses. This study is the first to our knowledge to show that smoke-induced reduction in C1q potentially underlies such T cell activation that likely involves autoreactive responses critical for the development of emphysema. Cigarette smoking, in turn, is linked to autoimmune phenomena, including rheumatoid arthritis and SLE (58, 59). Together, these findings indicate that proinflammatory cytokines can promote a relative or absolute reduction in functional C1q, which in turn can induce loss of tolerance to self in smokers.

Our report also documents the first use to our knowledge of macromolecular C1q that can prevent the development of smoke-induced emphysema despite active smoke exposure. Considering that symptomatic relief of airway obstruction is the only treatment available for management of smoke-induced lung inflammation, C1q and possibly pathways associated with its immune modulation are promising therapeutic candidates to prevent emphysema progression. In addition, given that a subset of patients with autoimmunity have neutralizing anti-C1q antibodies, it remains a critical objective to develop small molecules that recapitulate the function of C1q in augmenting Treg function under chronic inflammatory conditions.

Methods

Experimental model of emphysema. Mice (8 weeks old, females) were exposed to active smoke from commercial cigarettes (Marlboro 100 long, Marlboro; refs. 13, 36). Cigarettes are actively burned (approximately 4 to 5 min/cigarette) and smoke is carried through the cigarette filter and into the exposure chamber by intermittently forcing air (4 L/min) through the burning cigarette tip and into the combustion chamber. Intermittent cycles are designed to mimic puffing cycles of actual human smokers and to prevent asphyxiation of the mice. Puffing cycles are 5 seconds of active cigarette smoke followed by 25 seconds of forced air as controlled by a timer-controlled 2-way valve (Humphrey). Mice were given 4 cigarettes, 5 days a week for a total of 6 months, which approximates greater than 20 pack/year smoke exposure in humans (36).

Quantification and analysis of the experimental model of emphysema. Forty-eight hours following the last smoke exposure, mice were euthanized and BAL fluid was collected by instilling and withdrawing 0.8 mL of sterile PBS twice through the trachea. Total and differential cell counts in the BAL were determined with the standard hemocytometer and HEMA3 staining (Fisher Scientific) of 200 μL of BAL cytospin slide preparation. Cytokine and chemokine concentrations in the BAL were measured by Milliplex kit according to the manufacturer's instructions.

In some experiments, the lungs were either taken out for extracting single-cell suspension or were used for histology studies, whereby lungs were fixed with instillation of 4% paraformaldehyde solution via a tracheal cannula at 25 cmH_2O pressure followed by paraffin embedding. Embedded tissues were further cut into 5 micro slides and followed by H&E staining to assess lung structure and immune cell infiltration. MLI measurement was performed using established protocols (36). Briefly, 10 fields from the left lobe of the lungs (large airways and vessels were excluded) were randomly selected by an unbiased observer. Paralleled lines were placed on serial lung sections and MLI was calculated by multiplying the length and the number of lines per field, divided by the number of intercepts.

Human immune cell preparation and isolation. Human lung single-cell suspension was prepared as follows: briefly, fresh lung tissue was minced into 0.1-cm pieces in Petri dishes and treated with 2 mg/mL of collagenase D (Roche Pharmaceuticals) for 30 minutes at 37°C. Single cells were extracted by pressing digested lung tissue through a 40-μm cell strainer (BD Falcon), followed by red blood cell lysis using ACK lysis buffer (Sigma-Aldrich) for 3 minutes. PBMCs were isolated by Histopaque (Sigma-Aldrich) gradient centrifugation. Human $CD4^+$ T cells were selected from peripheral blood by labeling with bead-conjugated anti-CD4 (Miltenyi Biotec), followed by autoMACS positive selection. Human naive $CD4^+$ T cells were selected from peripheral blood by labeling with Human Naive $CD4^+$ T Cell Isolation Kit II (Miltenyi Biotec), followed by autoMACS negative depletion. Human $CD1a^+$ cells were selected from lung single-cell suspension by labeling with bead-conjugated anti-CD1a (Miltenyi Biotec), followed by autoMACS positive selection.

Mouse immune cell preparation and isolation. Mice lung, spleen, mLN, and pLN single-cell suspension was prepared by mincing the tissue through 40-μm cell strainer (BD Falcon), followed by red blood cell lysis using ACK lysis buffer (Sigma-Aldrich) for 3 minutes. Mouse splenic $CD4^+$ T cells were selected from peripheral splenocyte by labeling with bead-conjugated anti-CD4 (Miltenyi Biotec), followed by autoMACS positive selection. Mouse naive splenic $CD4^+$ T cells were selected from peripheral splenocyte by labeling with Mouse Naive $CD4^+$ T Cell Isolation Kit (Miltenyi Biotec), followed by autoMACS negative depletion. Mouse lung $CD11c^+$ dendritic cells were selected from lung single-cell suspension by labeling with bead-conjugated anti-CD11c (Miltenyi Biotec), followed by autoMACS.

In vitro T cell coculture and cytokine measurements. Mouse $CD4^+$ T cells from the spleen were cultured 3 days in vitro with lung APCs (10:1 ratio) in the presence of soluble anti–mouse CD3 (145-2C11, BD Biosciences, 1 μg/mL). Milliplex kit (Millipore) was used to measure concentrations of a selected group of cytokines (IL-4, IL-17, IL-6, IL-1β, IFN-γ) according to manufacturer's instructions. Alternatively, WT $CD4^+$ T cells were fixed and stained for intracellular transcription factor Foxp3 according to manufacturer's instruction (Foxp3 staining kit, eBioscience). *Foxp3-Gfp* transgenic $CD4^+$ T cells were directly stained with PE-CD4 (GK1.5, Biolegend) and APC-CD25 (PC61.5, eBioscience) to detect the Treg population.

Human $CD4^+$ T cells from PBMCs were cultured 3 days in vitro with monocyte-derived DCs (MDDCs) (10:1 ratio) in the presence of soluble anti–human CD3 (HIT3a, BD Biosciences, 1μg/mL). Milliplex kit (Millipore) was used to measure concentrations of a selected group of cytokines (IL-4, IL-17, IL-6, IL-1β, IFN-γ) according to manufacturer's instructions. Alternatively, T cells were fixed and stained for intracellular transcription factor Foxp3 according to manufacturer's instruction (Foxp3 staining kit, eBioscience).

In vitro differentiation of Treg and Th17 cells. Mouse naive $CD4^+$ T cells were isolated from splenocytes from WT mice or *Foxp3-Gfp* transgenic mice by autoMACS. After isolation, cells were counted and adjusted to a concentration of 2 to 2.25 × 10^6 cells/mL in complete medium (RPMI with 10% FBS, Pen-Strep 1:1000). Cells were stimulated with 1 μg/mL anti–mouse CD3 (145-2C11, BD Biosciences, 1 μg/mL), 1.5 μg/mL anti–mouse CD28 (37.51, BD Biosciences), 10 μg/mL ant–mouse IL-4 (11B11, BD Biosciences), 10 μg/mL anti–mouse IFN-γ (R4-6A2, BD Biosciences) and cultured in 24-well or 48-well tissue culture wells. For Treg condition, TGF-β (6 ng/mL) and IL-2 (50 U/mL) were supplemented in the culture; for Th17 differentiation, TGF-β (6 ng/mL), IL-6 (40 ng/mL) and IL-2 (50 U/mL) were supplemented in the culture with or without 20 μg/mL C1q (Complement Technology). Vehicle control $CD4^+$ T cells were isolated from WT mouse spleen and were then cultured for 3 days in the presence of anti-CD3 (145-2C11, BD Biosciences, 1 μg/mL), anti-CD28 (37.51, BD Biosciences), 10 μg/mL anti–mouse IL-4 (11B11, BD Biosciences), 10 μg/mL anti–mouse IFN-γ (R4-6A2, BD Biosciences) but did not receive Treg differentiation condition (TGF-β, anti–IL-4, anti–IFN-γ) with or without C1q. Cells were cultured for 3 days and harvested for intracellular transcription factor staining or stimulated to detect cytokine production. For transcription factor staining, Foxp3 was detected according to manufacturer's instruction (mouse Foxp3 staining kit, eBioscience). For the detection of RORγT, cells were fixed with fixation buffer from BD, permeabilized with 0.5% saponin, and stained with anti–mouse CD3 (145-2C11, BD Biosciences), anti–mouse CD4 (GK1.5, Biolegend), anti–mouse RORγT (B2D, eBioscience), and for analysis of intracellular cytokine.

Human naive $CD4^+$ T cells were isolated from PBMCs (Gulf Coast Blood Bank) by autoMACS. Cells were stimulated with Dynabeads Human T-Activator CD3/CD28 (ThermoFisher Scientific) and supplemented with TGF-β (6 ng/mL) and IL-2 (50 U/mL) in 24-well or 48-well tissue culture wells. Cells were cultured for 7 days and harvested for intracellular transcription factor staining.

Immunophenotype of single cells isolated from the lungs. RBC-free single-cell suspensions of the lung tissue were blocked with 2 μL/sample mouse Fc block and labeled with fluorescent anti-B220 (RA3-6B2, eBioscience), anti-CD11b (M1/70, BD Biosciences), anti-CD11c (HL3, BD Biosciences), and anti-Ly6C/G (RB6-8C5, BD Biosciences) antibodies, followed by detection of fluorescent signal using an LSRII (BD).

Alternatively, cells were stimulated with 10 ng/mL phorbol-myristate acetate (Sigma-Aldrich), and 200 ng/mL ionomycin supplemented with 10 ng/mL Brefeldin A (Sigma-Aldrich) overnight and were fixed with fixation buffer from BD, permeabilized with 0.5% saponin, and stained with Pacific Blue–conjugated anti–mouse CD3 (145-2C11, BD Biosciences), APC/Cy7–anti–mouse CD8 (53-6.7, Biolegend), PE/Cy–anti–mouse CD4 (GK1.5, Biolegend), APC–anti–mouse IFN-γ (XMG1.2, BD Biosciences), and PE–anti–mouse IL-17A (TC11-18H10, BD Biosciences) for analysis of intracellular cytokine production by flow cytometry.

Analysis of T cell activation status in peripheral lymphoid organs. RBC-free single-cell suspensions of the spleen, mesenteric lymph node, and draining lymph node were blocked with 2 μL/sample mouse Fc block and labeled with fluorescent anti-CD3 (145-2C11, BD Biosciences), anti-CD4 (GK1.5, Biolegend), anti-CD8 (53-6.7, Biolegend), anti-CD44 (IM7, Tonbo Biosciences), and anti-CD62L (MEL-14, Tonbo Biosciences) antibodies to detect the activation status of T cells, followed by detection of fluorescent signal using an LSRII (BD). Alternatively, RBC-free single-cell suspensions of the spleen, mesenteric lymph node, and draining lymph node were labeled with fluorescent anti-CD4 (GK1.5, Biolegend), anti-CD25 (PC61.5, eBioscience), anti-Foxp3 (3G3, eBioscence), anti-ICOS (C398.4A, Biolegend), and anti-PD1(29F.1A12, Biolegend) antibodies to detect Treg phenotype, followed by detection of fluorescent signal using an LSRII (BD).

mRNA isolation and quantitative PCR. Total cellular mRNA was extracted by the following protocol: Cell pellets were treated with TRIzol (Invitrogen) and then extracted by adding chloroform (Sigma-Aldrich). mRNA was then deposited with isopropanol (Sigma-Aldrich) and washed with 70% alcohol (Sigma-Aldrich). The concentration of mRNA was measured using NanoDrop 2000 (ThermoFisher Scientific).

Quantitative PCR was performed by 1-step real-time reverse transcription PCR to determine the relative gene expression using the ABI Perkin Elmer Prism 7500 Sequence Detection System (Applied Biosystems). All gene probes, *Mmp9* (Mm00600164_g1), *Mmp12* (Mm00500554_m1), *Il6* (Mm00446190_m1), *Il1beta* (Mm00434228_m1), *C1qa* (Mm00432142_m1), *Cd274* (Mm00452054_m1), *Itgae/Cd103* (Mm00434443_m1), and human *C1QA* (Hs00706358_s1) were purchased from Applied Biosystems. All data were normalized to *18S* ribosomal RNA (Hs99999901_s1) expression.

siRNA-mediated knockdown of C1q expression. siRNA for C1QA was purchased from Sigma-Aldrich (MISSION esiRNA human C1QA and scramble siRNA). Human MDDCs were transfected using human DC Nucleofection kit (Lonza) according to manufacturer's instructions. Sham and scrambled siRNA were used as controls. MDDCs pretreated with siRNA were incubated overnight, washed with medium, and then cocultured with human $CD4^+$ T cells.

Quantification of C1q in human plasma and lung tissue lysate. The concentrations of C1q protein in heparinized human plasma and lung tissue lysate were quantified after samples were diluted (PBST with 1% BSA), using Sandwich ELISA. Briefly, Immulon ELISA plates were coated with 1:200 monoclonal anti-human C1q (Abcam, ab71940) in carbonate buffer overnight at 4°C. Plates were washed with PBST 3 times and blocked in 3% BSA in PBST for 1 hour at room temperature. Samples and standards were diluted and added to the plates. After 2 hours of incubation at room temperature, plates were washed with PBST 3 times. Polyclonal Rb anti-hC1q (Abcam, Ab20539; 1:2000) was added to detect C1q. After a 1-hour incubation at room temperature, plates were washed 5 times with PBST and 1:5000 goat anti-rabbit-biotin secondary antibody (Vector, BA-1000) was added to amplify the signal. After a 1-hour incubation at room temperature, plates were washed 5 times with PBST and developed by BD OptEIA TMB substrate (BD). Final readout was detected by absorbance at 450 nm.

Transcriptomic analysis. Gene expression data was normalized using the R statistical system. A principal component analysis was performed within R and visualization was generated using the python visualization library Matplotlib. Differential gene expression was assessed using a 2-sided *t* test using R; significance was achieved for adjusted *P* value less than 0.01; fold change greater than 1.4 upregulated/downregulated. Differentially expressed genes were visualized using hierarchical clustering via the Python Matplotlib library. For each comparison, a rank file was generated using the log2 fold change of all detected genes, and gene set enrichment analysis (GSEA) analysis was performed using the GSEA software package (60). The data can be accessed at https://figshare.com/articles/Cigarette_smoke-induced_reduction_of_C1q_promotes_emphysema/8088110.

Statistics. All statistical analyses were performed with Prism software (GraphPad Software). All data points in this study are shown as the mean and the error bars represent SEM unless otherwise indicated. For the comparison of BAL cellularity and gene expression from the air- and smoke-exposed mice, we used the 2-tailed Student's *t* test or 1-way ANOVA test and Bonferroni's correction for multiple comparisons. The C1q concentrations were analyzed using the Mann-Whitney nonparametric test. Linear regression was performed to determine the correlation between C1q mRNA expression and lung disease as measured by the FEV/FVC ratios. For the comparison of CT quantification of air- and smoke-exposed mice, the 2-way ANOVA test was used. We considered differences significant when the *P* value was equal to or less than 0.05.

Study approval. Plasma, lung tissue, or PBMCs were collected from a total of 134 non-atopic current or former smokers who were recruited into our ongoing COPD study. Emphysema was diagnosed based on radiographic findings on chest CT available at the time of lung tissue collection. COPD was diagnosed

Table 1. Demographics

Characteristics	Control	Emphysema
No. (male)	53 (22)	81 (69)[A]
Age (mean ± SD)	54 ± 10	64 ± 10[B]
Pulmonary Function		
% FEV_1 (mean ± SD)	92 ± 15	58 ± 22[B]
% FEV_1/FVC (mean ± SD)	80 ± 11	58 ± 16[B]
Smoking Status		
No. Former	20	46
No. Current	23	35
No. Never	10	0
PPY (mean ± SD)	51 ± 37	68 ± 31

FEV_1, forced expiratory volume in 1 second; FVC, forced vital capacity. PPY, year multiplied by number of packs of cigarettes per day. [A]$P < 0.001$, as determined by the Fisher's exact test. [B]$P < 0.0001$, as determined by the Mann-Whitney test.

according to the criteria recommended by the NIH/WHO workshop summary (61). Smoking 1 pack of cigarettes per day each year is defined as 1 pack-year. Subjects were recruited from the chest or surgical clinics at the Baylor Clinic, Methodist, and Michael E. DeBakey Houston VAMC hospitals. The patients had no history of allergy or asthma, had not received oral or systemic corticosteroids, and were free of acute symptoms suggestive of upper or lower respiratory tract infection during the last 6 weeks. Studies were approved by the Institutional Review Board at Baylor College of Medicine, and informed consents were obtained from all patients. Full patient demographics data are provided in Table 1.

WT mice (females, C57BL/6J background) were purchased from the Jackson Laboratories. *C1qa*$^{-/-}$ mice were provided by Yi Xu from the Institute of Biosciences and Technology, Texas A&M Health Science Center with the permission from Marina Botto from King's College, London, United Kingdom. Littermate WT mice (females, C57BL/6J background) bred in the same facility were used as controls. *Foxp3-Gfp* transgenic mice were purchased from the Jackson Laboratories. *Foxp3-Gfp* mice were crossed to *C1qa*$^{-/-}$ mice for 2 generations and mice in the F2 generation were screened for both *Foxp3-Gfp* and *C1qa*$^{-/-}$ genotype. Then mice with both *Foxp3-Gfp* positivity and C1qa deletion were chosen as breeders for further mice propagation. All mice were bred in the transgenic animal facility at Baylor College of Medicine. The hypomorphic nature of the Foxp3-GFP transgenic mice was noted in previous study (62), thus littermate Foxp3-*Gfp* mice were used as control animals. All experiments were approved by the Institutional Animal Care and Use Committee of Baylor College of Medicine.

Author contributions

XY carried out experiments, collected and analyzed data, and assisted with manuscript preparation. CYC, RY, MS, BHG, MCM, and LZS assisted with data collection and smoke exposure experiments. SP, LZS, and LC assisted with human tissue studies. RK and CC assisted with RNA-seq data analysis. RDR, RW, and HKE provided critical comments and experimental suggestions. XY, DBC, GD, and FK designed experiments, analyzed data, and prepared the manuscript.

Acknowledgments

This work was in part supported by NIH R01 AI135803-01 to FK and DC; VA Merit CX000104 and NIH R01 ES029442-01 to FK; NIH HL140398 to DC; and by the Cytometry and Cell Sorting Core at Baylor College of Medicine with funding from the NIH (AI036211, CA125123, and RR024574) and the expert assistance of Joel M. Sederstrom. This work was supported by CPRIT RP160283 - Baylor College of Medicine Comprehensive Cancer Training Program.

Address correspondence to: Farrah Kheradmand or David B. Corry, Address, One Baylor Plaza, Baylor College of Medicine, Houston, Texas 77030, USA. Phone: 713.798.8622; Email: farrahk@bcm.edu (FK). Phone: 713.798.8740; Email: dcorry@bcm.edu (DC).

1. Vestbo J. COPD: definition and phenotypes. *Clin Chest Med*. 2014;35(1):1–6.
2. Labaki WW, Martinez CH, Han MK. COPD in 2016: some answers, more questions. *Lancet Respir Med*. 2016;4(12):941–943.
3. You R, et al. Nanoparticulate carbon black in cigarette smoke induces DNA cleavage and Th17-mediated emphysema. *Elife*. 2015;4:e09623.
4. Lu W, et al. The microRNA miR-22 inhibits the histone deacetylase HDAC4 to promote T(H)17 cell-dependent emphysema. *Nat Immunol*. 2015;16(11):1185–1194.
5. Barnes PJ. Cellular and molecular mechanisms of asthma and COPD. *Clin Sci*. 2017;131(13):1541–1558.
6. Polverino F, Celli B. The challenge of controlling the COPD epidemic: unmet needs. *Am J Med*. 2018;131(9S):1–6.
7. Kheradmand F, Shan M, Xu C, Corry DB. Autoimmunity in chronic obstructive pulmonary disease: clinical and experimental evidence. *Expert Rev Clin Immunol*. 2012;8(3):285–292.
8. Lee SH, et al. Antielastin autoimmunity in tobacco smoking-induced emphysema. *Nat Med*. 2007;13(5):567–569.
9. Bhavani S, et al. Clinical and immunological factors in emphysema progression. five-year prospective longitudinal exacerbation study of chronic obstructive pulmonary disease (LES-COPD). *Am J Respir Crit Care Med*. 2015;192(10):1171–1178.
10. Xu C, et al. Autoreactive T cells in human smokers is predictive of clinical outcome. *Front Immunol*. 2012;3:267.
11. Rabinovich RA, et al. Circulating desmosine levels do not predict emphysema progression but are associated with cardiovascular risk and mortality in COPD. *Eur Respir J*. 2016;47(5):1365–1373.
12. Shan M, et al. Lung myeloid dendritic cells coordinately induce TH1 and TH17 responses in human emphysema. *Sci Transl Med*. 2009;1(4):4ra10.
13. Shan M, et al. Cigarette smoke induction of osteopontin (SPP1) mediates T(H)17 inflammation in human and experimental emphysema. *Sci Transl Med*. 2012;4(117):117ra9.
14. Maeno T, Houghton AM, Quintero PA, Grumelli S, Owen CA, Shapiro SD. $CD8^+$ T cells are required for inflammation and destruction in cigarette smoke-induced emphysema in mice. *J Immunol*. 2007;178(12):8090–8096.
15. Klareskog L, Gregersen PK, Huizinga TW. Prevention of autoimmune rheumatic disease: state of the art and future perspectives. *Ann Rheum Dis*. 2010;69(12):2062–2066.
16. Long H, Yin H, Wang L, Gershwin ME, Lu Q. The critical role of epigenetics in systemic lupus erythematosus and autoimmunity. *J Autoimmun*. 2016;74:118–138.
17. Pertovaara M, et al. Autoimmunity and atherosclerosis: the presence of antinuclear antibodies is associated with decreased carotid elasticity in young women. The Cardiovascular Risk in Young Finns Study. *Rheumatology (Oxford)*. 2009;48(12):1553–1556.
18. Gregersen PK, Olsson LM. Recent advances in the genetics of autoimmune disease. *Annu Rev Immunol*. 2009;27:363–391.
19. Núñez B, et al. Anti-tissue antibodies are related to lung function in chronic obstructive pulmonary disease. *Am J Respir Crit Care Med*. 2011;183(8):1025–1031.
20. Packard TA, Li QZ, Cosgrove GP, Bowler RP, Cambier JC. COPD is associated with production of autoantibodies to a broad spectrum of self-antigens, correlative with disease phenotype. *Immunol Res*. 2013;55(1-3):48–57.
21. Zipfel PF, Skerka C. Complement regulators and inhibitory proteins. *Nat Rev Immunol*. 2009;9(10):729–740.
22. Lubbers R, van Essen MF, van Kooten C, Trouw LA. Production of complement components by cells of the immune system. *Clin Exp Immunol*. 2017;188(2):183–194.
23. Yuan X, et al. Activation of C3a receptor is required in cigarette smoke-mediated emphysema. *Mucosal Immunol*. 2015;8(4):874–885.
24. West EE, Kolev M, Kemper C. Complement and the regulation of T cell responses. *Annu Rev Immunol*. 2018;36:309–338.
25. Raedler H, Heeger PS. Complement regulation of T-cell alloimmunity. *Curr Opin Organ Transplant*. 2011;16(1):54–60.
26. Scott D, Botto M. The paradoxical roles of C1q and C3 in autoimmunity. *Immunobiology*. 2016;221(6):719–725.
27. Son M, Diamond B, Santiago-Schwarz F. Fundamental role of C1q in autoimmunity and inflammation. *Immunol Res*. 2015;63(1–3):101–106.
28. Wisnieski JJ, et al. Hypocomplementemic urticarial vasculitis syndrome. Clinical and serologic findings in 18 patients. *Medicine (Baltimore)*. 1995;74(1):24–41.
29. Mehta P, et al. SLE with C1q deficiency treated with fresh frozen plasma: a 10-year experience. *Rheumatology (Oxford)*. 2010;49(4):823–824.
30. Ghebrehiwet B, Hosszu KH, Peerschke EI. C1q as an autocrine and paracrine regulator of cellular functions. *Mol Immunol*. 2017;84:26–33.
31. Thielens NM, Tedesco F, Bohlson SS, Gaboriaud C, Tenner AJ. C1q: A fresh look upon an old molecule. *Mol Immunol*. 2017;89:73–83.
32. Fonseca MI, et al. Cell-specific deletion of C1qa identifies microglia as the dominant source of C1q in mouse brain. *J Neuroinflammation*. 2017;14(1):48.
33. Botto M, Kirschfink M, Macor P, Pickering MC, Würzner R, Tedesco F. Complement in human diseases: Lessons from complement deficiencies. *Mol Immunol*. 2009;46(14):2774–2783.
34. Tsai CL, et al. Factors associated with progression of emphysema quantified by CT scan in ever smokers: the 5-year Prospective LES-COPD Study. *Am J Respir Crit Care Med*. 2014;189:A5105.
35. Yamada M, et al. Complement C1q regulates LPS-induced cytokine production in bone marrow-derived dendritic cells. *Eur J Immunol*. 2004;34(1):221–230.
36. Shan M, et al. Agonistic induction of PPARγ reverses cigarette smoke-induced emphysema. *J Clin Invest*. 2014;124(3):1371–1381.
37. Yawn BB, et al. The 2017 Update to the COPD Foundation COPD Pocket Consultant Guide. *Chronic Obstr Pulm Dis*. 2017;4(3):177–185.
38. Latz E, Xiao TS, Stutz A. Activation and regulation of the inflammasomes. *Nat Rev Immunol*. 2013;13(6):397–411.
39. Ohta A, Kini R, Ohta A, Subramanian M, Madasu M, Sitkovsky M. The development and immunosuppressive functions of CD4(+) CD25(+) FoxP3(+) regulatory T cells are under influence of the adenosine-A2A adenosine receptor pathway. *Front Immunol*. 2012;3:190.
40. Ohta A, Sitkovsky M. Extracellular adenosine-mediated modulation of regulatory T cells. *Front Immunol*. 2014;5:304.
41. Sitkovsky MV. T regulatory cells: hypoxia-adenosinergic suppression and re-direction of the immune response. *Trends Immunol*. 2009;30(3):102–108.

42. Fantini MC, Dominitzki S, Rizzo A, Neurath MF, Becker C. In vitro generation of $CD4^+$ $CD25^+$ regulatory cells from murine naive T cells. *Nat Protoc*. 2007;2(7):1789–1794.
43. Bordin S, Tan X. C1q arrests the cell cycle progression of fibroblasts in G(1) phase: role of the cAMP/PKA-I pathway. *Cell Signal*. 2001;13(2):119–123.
44. Hong Q, et al. Complement C1q activates tumor suppressor WWOX to induce apoptosis in prostate cancer cells. *PLoS One*. 2009;4(6):e5755.
45. Kaur A, et al. Human C1q Induces Apoptosis in an Ovarian Cancer Cell Line. *Front Immunol*. 2016;7:599.
46. Mascarell L, et al. The regulatory dendritic cell marker C1q is a potent inhibitor of allergic inflammation. *Mucosal Immunol*. 2017;10(3):695–704.
47. Ricklin D, Hajishengallis G, Yang K, Lambris JD. Complement: a key system for immune surveillance and homeostasis. *Nat Immunol*. 2010;11(9):785–797.
48. Martin M, Blom AM. Complement in removal of the dead - balancing inflammation. *Immunol Rev*. 2016;274(1):218–232.
49. Ogden CA, et al. C1q and mannose binding lectin engagement of cell surface calreticulin and CD91 initiates macropinocytosis and uptake of apoptotic cells. *J Exp Med*. 2001;194(6):781–795.
50. Verneret M, et al. Relative contribution of c1q and apoptotic cell-surface calreticulin to macrophage phagocytosis. *J Innate Immun*. 2014;6(4):426–434.
51. Ramirez-Ortiz ZG, et al. The scavenger receptor SCARF1 mediates the clearance of apoptotic cells and prevents autoimmunity. *Nat Immunol*. 2013;14(9):917–926.
52. Benoit ME, Clarke EV, Morgado P, Fraser DA, Tenner AJ. Complement protein C1q directs macrophage polarization and limits inflammasome activity during the uptake of apoptotic cells. *J Immunol*. 2012;188(11):5682–5693.
53. Clarke EV, Weist BM, Walsh CM, Tenner AJ. Complement protein C1q bound to apoptotic cells suppresses human macrophage and dendritic cell-mediated Th17 and Th1 T cell subset proliferation. *J Leukoc Biol*. 2015;97(1):147–160.
54. Son M, Santiago-Schwarz F, Al-Abed Y, Diamond B. C1q limits dendritic cell differentiation and activation by engaging LAIR-1. *Proc Natl Acad Sci U S A*. 2012;109(46):E3160–E3167.
55. Leffler J, Bengtsson AA, Blom AM. The complement system in systemic lupus erythematosus: an update. *Ann Rheum Dis*. 2014;73(9):1601–1606.
56. Rutgers SR, et al. Ongoing airway inflammation in patients with COPD who do not currently smoke. *Thorax*. 2000;55(1):12–18.
57. Lapperre TS, et al. Relation between duration of smoking cessation and bronchial inflammation in COPD. *Thorax*. 2006;61(2):115–121.
58. Aho K, Heliövaara M. Risk factors for rheumatoid arthritis. *Ann Med*. 2004;36(4):242–251.
59. Arnson Y, Shoenfeld Y, Amital H. Effects of tobacco smoke on immunity, inflammation and autoimmunity. *J Autoimmun*. 2010;34(3):J258–J265.
60. Subramanian A, et al. Gene set enrichment analysis: a knowledge-based approach for interpreting genome-wide expression profiles. *Proc Natl Acad Sci U S A*. 2005;102(43):15545–15550.
61. NIH/WHO. NIH/WHO diagnostic COPD criteria. https://www.nhlbi.nih.gov/health-topics/copd.
62. Bettini ML, et al. Loss of epigenetic modification driven by the Foxp3 transcription factor leads to regulatory T cell insufficiency. *Immunity*. 2012;36(5):717–730.